J. Electrochem. Sci. Eng. **12(5)** (2022) 923-935; https://dx.doi.org/10.5599/jese.1259

Open Access : : ISSN 1847-9286
https://pub.iapchem.org/ojs/index.php/JESE

Original scientific paper

The effect of process parameters on microstructure and corrosion behavior of AISI 4140 steel modified by pulse plasma treatment

Yıldız Yaralı Özbek✉ and Ayşe Şükran Demirkiran

Sakarya University, Engineering Faculty, Department of Metallurgy and Materials Engineering, Esentepe Campus, 54187, Sakarya, Turkey and Sakarya University, Research, Development and Application Center (SARGEM), Sakarya, Turkey

Corresponding author: ✉*yyarali@sakarya.edu.tr; Tel +902642955619*

Received: January 27, 2022; Accepted: July 19, 2022; Published: September 14, 2022

Abstract

The pulse plasma system is a surface modification method applied to steel samples. In the present study, the effect of the nozzle distance and pulse number parameters were investigated on the modification process. AISI 4140 steel was preferred as the substrate for modification. In this system, the battery capacity and voltage were constant, and, were selected as 800 mF and 3000 V, respectively. The AISI 4140 steel samples were modified by applying 5, 10, and 15 pulses with 40, 50 and 60 mm nozzle distance. The molybdenum consumable electrode was used during the process. The modified surfaces were examined by optical and scanning electron microscope (SEM) and analyzed by X-ray diffractometer (XRD). Vickers microhardness on the cross-section surface of the samples was measured under a load of 50 g for 15 s. Finally, the specimens were exposed to corrosion in 0.5 M NaCl solution. Corrosion tests were realized using the potentiodynamic polarization method. A modified layer on the steel was determined to consist of two layers, the compound layer and the diffusion layer. It was observed that the structure and thickness of the modified layer affect by pulse number and nozzle distance. New phases such as Fe_2N, FeN, MoN, and γ-Fe in the modified layer have occurred. The hardness value of the treated sample has risen about 4-5 times than the untreated, depending on applied process parameters. In general, the pulse plasma treatment has improved the corrosion resistance of treated samples. It was observed that while intergranular corrosion has formed on the unmodified surface, pitting corrosion has appeared on the unmodified surfaces.

Keywords

Surface, hardness, coating, molybdenum

Introduction

Technological advances compel the use of materials in extremely aggressive conditions such as corrosive atmospheres and/or abrasive wear situations [1,2]. In recent years, a new process for surface modification of materials has emerged based on pulsed power beams [3,4].

The pulse plasma process is especially a method used to improve the surface properties of work pieces of tool steels [2-5]. The pulse plasma process is described by the formation of high-gradient temperature fields concentrated in heat. Compared with conventional surface treatment techniques, the pulse process has advantages in many ways [5,6]. For example, the surfaces of complex-shaped parts can be easily modified without residual tension stress. Also, the pulse treatment is occurred in a very short time and easily.

High energy density transferred to the surface by plasma pulse leads to ultra-high-speed heating followed by very fast cooling due to heat evacuation inward the bulk of substrate [7]. The result is a modification of the near-surface layer, *i.e.,* changing its structure and properties [7-9].

The coating is formed by the vapors of inner chamber material as well as by the vapor and micro-droplets of cathode material which are the result of high-current discharge inside the chamber. The cathode material dramatically influences the chemical composition and the structure of the coating. The consumable electrode (molybdenum or tungsten) is used to cathode plasma accelerators [6-19]. This situation facilitates the cathode surface melting, which leads to an increase in mass transfer by a micro-droplet fraction.

When started by pulse treatment, a very rapid melt and solidification occur on the surface layer of samples. It is found that the pulse plasma process may lead to metastable structure in coating resulting from fast crystallization of plasma transferred material (*i.e.,* "solute trapping" effect [20,21]). Also, the high rates of ions can accelerate the formation of microcrystalline surface layers. During process time, the compound zone (white layer) and the diffusion zone on the modified layer occur. High surface residual stresses (compression stress) are generated in the compound zones, resulting from chemical composition gradients, stress fields around precipitates, volume changes, and thermal effects [5,6,8].

The source of alloying elements is a consumable electrode such as Mo and W on treatment. These ionized products of electrode and nitrogen gases are used to modify the surface. These ionized products are dissolved or precipitated as iron-nitrides, alloys on the surface. The modified layers exhibit high hardness due to dispersed alloy nitrides and new phases in the matrix. With this development, the mechanical behaviors of the sample can be changed and improved [6,8,11].

Depending on pulse plasma parameters, different plasma chemical reactions may occur, leading to a specific phase state of the coating. The process parameters affect the steel surfaces' final structure and mechanical properties. Among these parameters, controlling gas diffusion through the nozzle distance, the number of pulses, and the battery capacity are the most critical parameters. The proper combination of these parameters would provide the best surface properties and decrease the processing time as an essential economic factor.

The main aim of this work is to examine the microstructure, hardness, and corrosion properties of AISI 4140 steel surface modified by pulse-plasma treatment realized by applying different parameters.

Experimental

Preparation of the samples and modification process

In the present study, AISI 4140 steel which is very cheap and is widely used in the industry, was selected as the substrate for surface modification. The chemical composition of AISI 4140 steel is presented in Table 1. Firstly, the specimens were cut out as square bars and subsequently machined and metallographically prepared to obtain the desired shape and surface roughness. The sample surfaces were sanded from 120 to 1200 mesh with SiC sandpaper and polished with 0.05 µm alumina solution. The pulse plasma process was applied on clean surfaces prepared. The molybdenum (Mo) consumable electrode was used in this treatment.

In the pulse plasma system, seen in Figure 1, the 3000 V high voltage and 800 mF capacity of the capacitor bank were selected. The power density of the heat flow is 10^7 W cm^{-2}. This situation leads to evaporation of the dielectric walls of the discharge chamber and melting and evaporating of the electrodes (mainly the molybdenum). Thus, plasma jet formation occurs. The molten cathode material is carried away by the gas stream and, possibly, partially enters the inner surface of the discharge chamber, which leads to its intense heating at the points of contact with the liquid metal. The high-speed shooting shows that when a gas outflows from the chamber within a few milliseconds, ejection of liquid metal drops occurs. Following the surface layer's quick heating (10^5 to 10^7 K s^{-1}), intensive cooling is ensured by rapidly removing heat from the mass. The parameters used in the pulse plasma process are presented in Table 2.

Table 1. *Chemical composition of the AISI 4140 steel used as the substrate for surface modification*

Element	C	Si	Mn	P	S	Cr	Mo	Fe
Content, wt.%	0.39	0.30	0.80	0.035	0.015	0.90	0.13	Balance

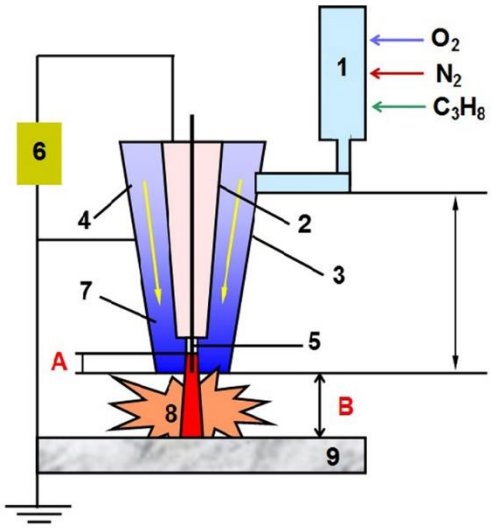

Figure 1*. Schematic presentation of the pulsed-plasma modification system*

Table 2*. The parameters of pulse plasma treatment and the sample codes*

Parameters	Sample code								
	1	2	3	4	5	6	7	8	9
Nozzle distance, mm	40	40	40	50	50	50	60	60	60
Number of pulses	5	10	15	5	10	15	5	10	15

Characterization of the modified surface

After the pulse plasma treatments, all specimens were sanded with different mesh number sand-papers, polished with 3 µm diamond paste, and etched using the 2 % nital solution. The cross-section microstructures were examined using an optical microscope. Besides, the morphology of pulse plasma-treated samples was observed by SEM (JEOL-JSM 6060 LV) and analyzed with a RIGAKU D/MAX/2200/PC brand device operating with Cu-Kα (λ = 0.154056 nm) radiation. Vickers micro-hardness tests (Shimadzu Brand) on the polished cross-section surface of the samples were performed under a load of 50 g ($HV_{0.050}$) for 15 sec. Measurements were made as many times as possible from different parts of the specimen, and the arithmetic mean of the obtained values was taken.

Corrosion tests of the modified surface

The untreated and the samples modified with different process parameters were cleaned in ethanol as ultrasonic, washed with deionized water, and finally dried with compressed air. 0.5 M

NaCl (Merck Company) solution was prepared with distilled water. The specimens were isolated so that only the sample surface area of 0.8023 cm^2 was provided to contact with the solution. Corrosion tests were realized using the potentiodynamic polarization method. All electrochemical measurements were performed using Gamry Instruments PCl4/750 potentiostat/galvanostat/ZRA electrochemical analyzer system. An Ag/AgCl/KCl electrode was used as a reference electrode, and a graphite electrode was used as a counter electrode in corrosion experiments using a traditional three-electrode system. The schematic representation of the corrosion cell used is presented in Figure 2.

All potentiodynamic polarization measurements were carried out at room temperature, a scanning rate of 5 mV s^{-1}, and a scan range from -1 to +1 V. Data were analyzed using the Gamry EChem Analyst software package. The corrosion current (I_{corr}), corrosion potential (E_{corr}), and corrosion rate (R_{corr}) values were determined with Tafel extrapolation, which is a mathematical technique. Equation (1) is used to determine the corrosion rate:

$$R_{corr} = \frac{I_{corr}\, K\, EW}{dA} \quad (1)$$

where, R_{corr} / mm $year^{-1}$ is the corrosion rate, I_{corr} / µA is the corrosion current, K is a constant (0.00327 mm g $year^{-1}$ μA^{-1} cm^{-1}), EW / g is the equivalent weight, A / cm^2 is the sample area and d / g cm^{-3} is the density [10].

All the tests were repeated three times to ensure the accuracy and stability of the experimental data. The mean value and standard deviation of the results were calculated. Finally, the corrosion region of the samples was examined by SEM (JEOL-JSM 6060 LV).

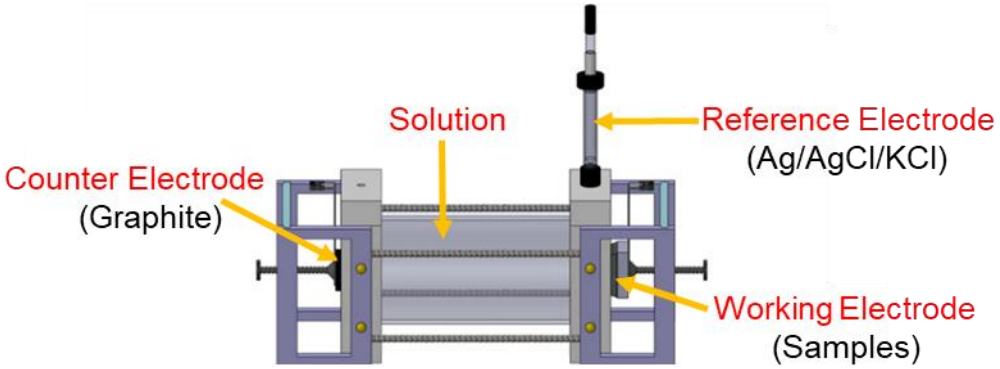

***Figure 2**. The schematic representation of the corrosion cell used*

Results and discussion

Microstructural characterization of the modified surfaces

SEM micrographs taken from the cross-section of the steel modified by applying 5, 10, and 15 pulses with 60 mm nozzle distance are presented in Figure 3a-c.

Microstructural analyses show that morphological changes on the surface resulting from high power energy and thermal effect occur [8], and pulse plasma application resulted in micrographs having different contrast layers. It is seen that the modified layer consists of two layers, the compound layer and the diffusion layer, the pulse number affected the modification layer, and the thickness of the layer modified increased with the increase in pulse number. For example, the modified layer thickness of the sample subjected to 5 pulses with 60 mm nozzle distance is 34.26 µm, while the modified layer thickness of the sample subjected to 15 pulses with 60 mm nozzle distance was measured as 48.06 µm (Figures 4 a and 4b). Other researchers have reported similar results [1,2,9,11].

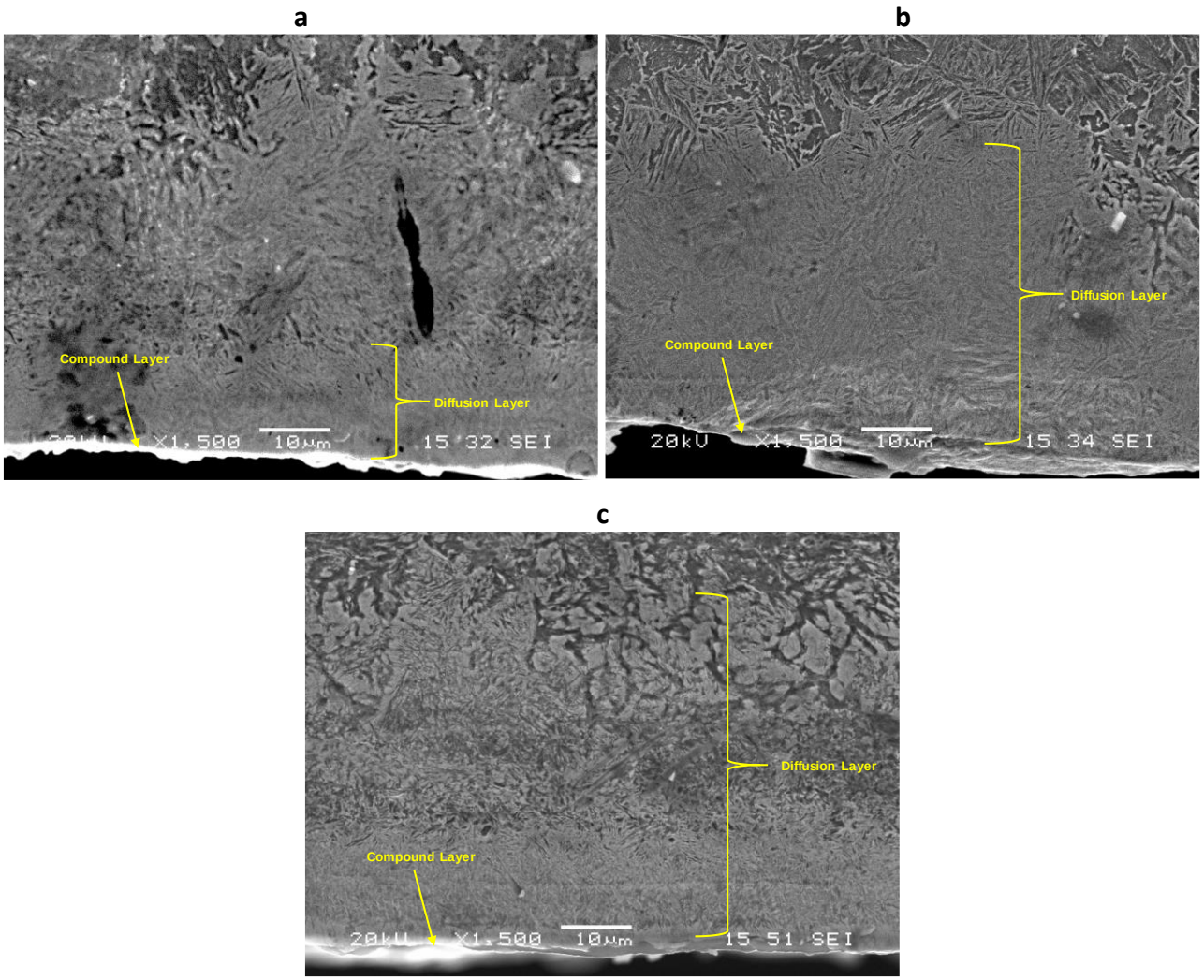

***Figure 3**. SEM micrographs taken from the cross-section of the steel modified by applying (a) 5, (b) 10, and (c) 15 pulses with 60 mm nozzle distance*

SEM micrographs taken from the cross-section of the steel modified by applying 10 pulses with 40, 50, and 60 mm nozzle distances are presented in Figure 5a-c. Similarly, like pulse number, the nozzle distance also affects the modification layer, and the thickness of the layer modified increases with the increase in nozzle distance.

At the same time, the rapid solidification induced by pulse plasma leads to the formation of metastable structures, superfine grains, and fine dendritic structures in the modified layer [4,8,11]. It is known that instability of the surface structure increases with increasing diffusion of atoms, rapid heating and cooling results in the generation of high dislocation densities, fine grain, and defects on the surfaces of the work pieces [7,9,11-13]. The ε-nitrides develop on top of the γ_1-nitrides and build a layer with thinner grains. Figure 6 presents an SEM micrograph showing the dendritic structure taken from the cross-section of the steel modified by applying 10 pulses with a 50 mm nozzle distance. Some dendrites contain martenzite, which indicates a high cooling rate during solidification.

Cheng *et al.* [13] have stated that the interdendrites were characterized by long primary and secondary arms, and the secondary arm spacing was less than 0.5 µm. Zhang, Guana, and Uglov have also reported similar results for the modification layer [13-17].

On the other hand, the fact that no cracks were seen in the micrographs indicates that the severe cooling of the pulse plasma modified specimens did not cause noticeable micro defects.

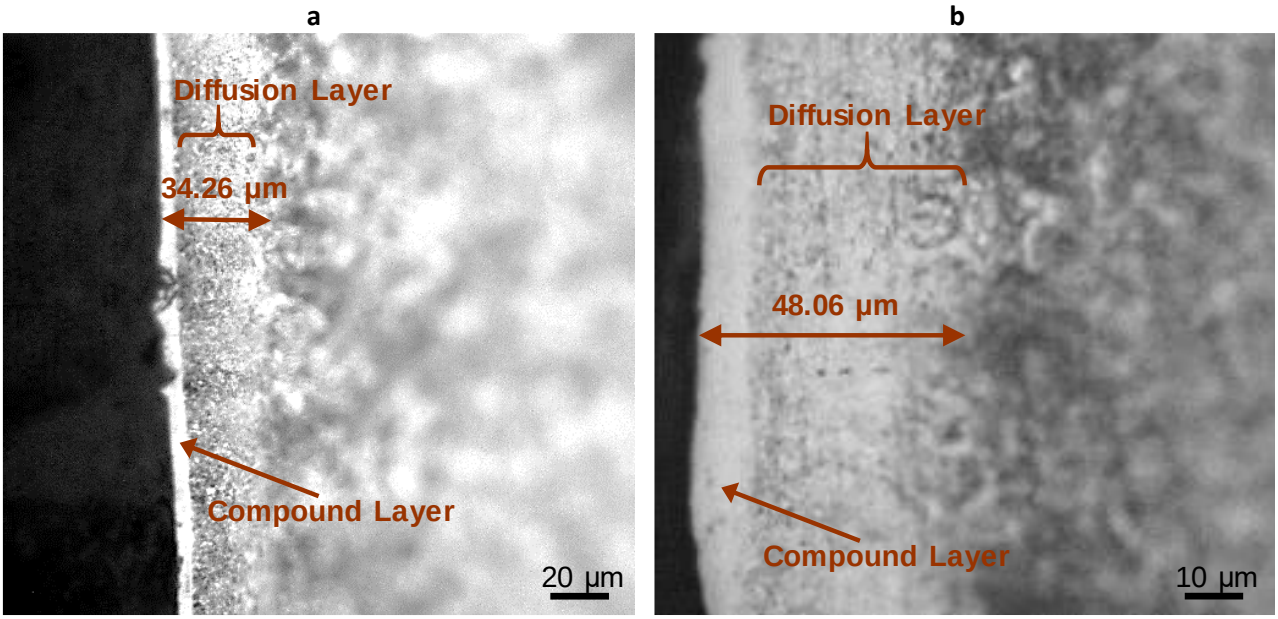

Figure 4. *Optical micrographs taken from the cross-section of the steel modified by applying a - 5, and b - 15 pulses with 60 mm nozzle distance*

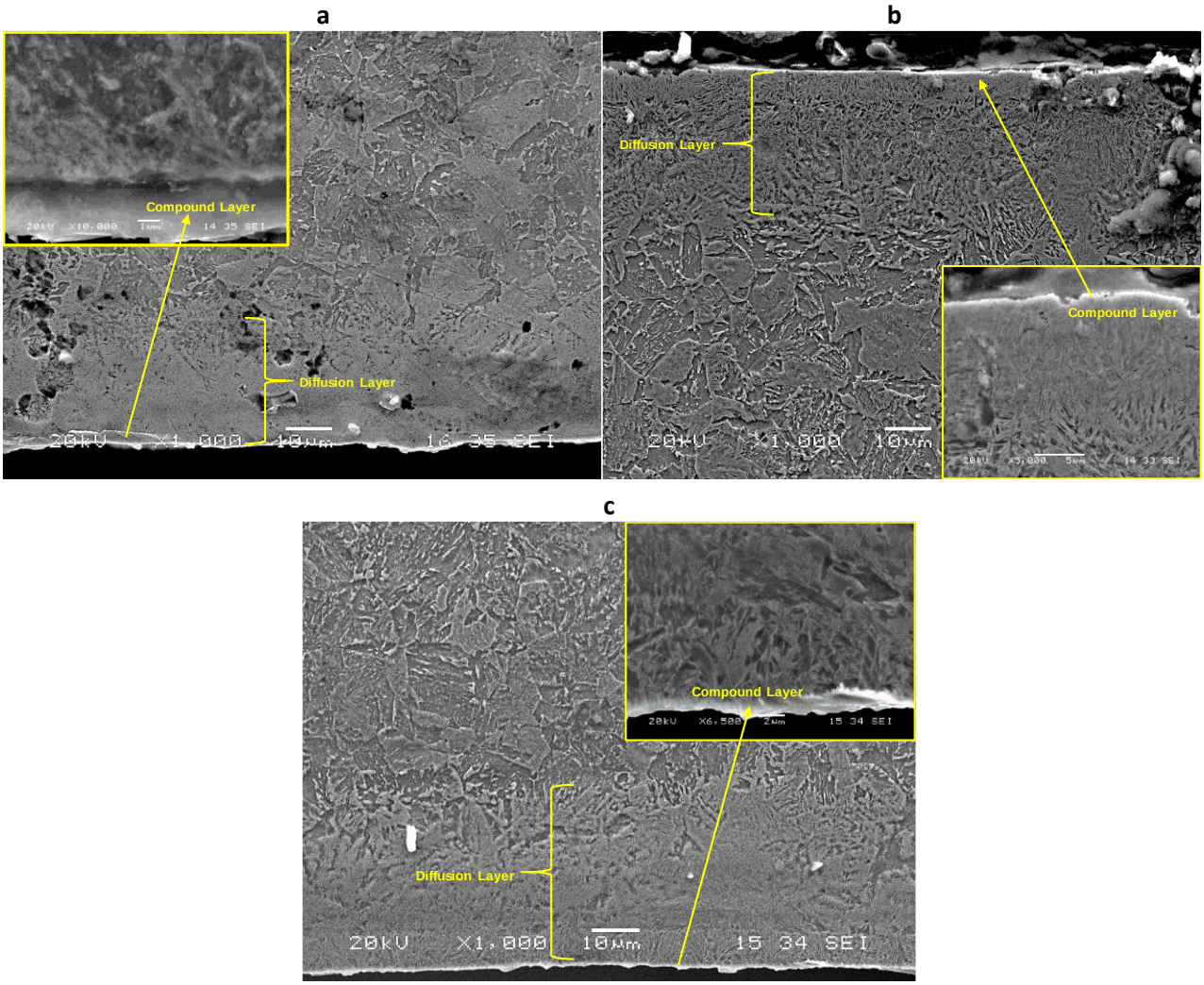

Figure 5. *SEM micrographs taken from the cross-section of the steel modified by applying 10 pulses with a - 40, b - 50 and c - 60 mm nozzle distances*

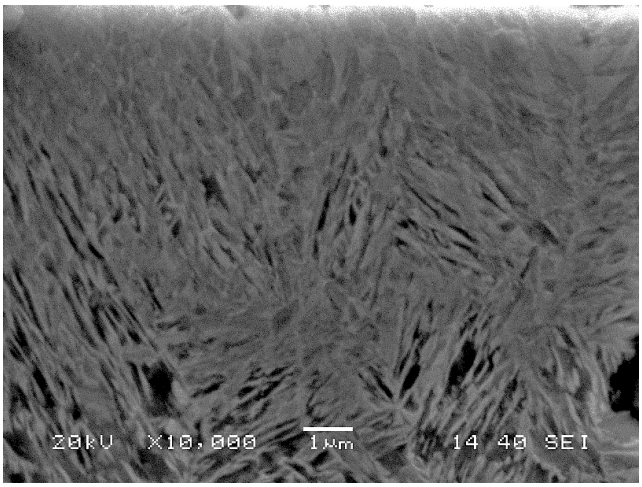

Figure 6. *SEM micrograph showing the dendritic structure taken from the cross-section of the steel modified by applying 10 pulses with a 50 mm nozzle distance*

Phase analyses of the samples

XRD analyses were performed to identify the phase content of the unmodified and the modified surfaces. The results obtained are presented in Figure 7a-c.

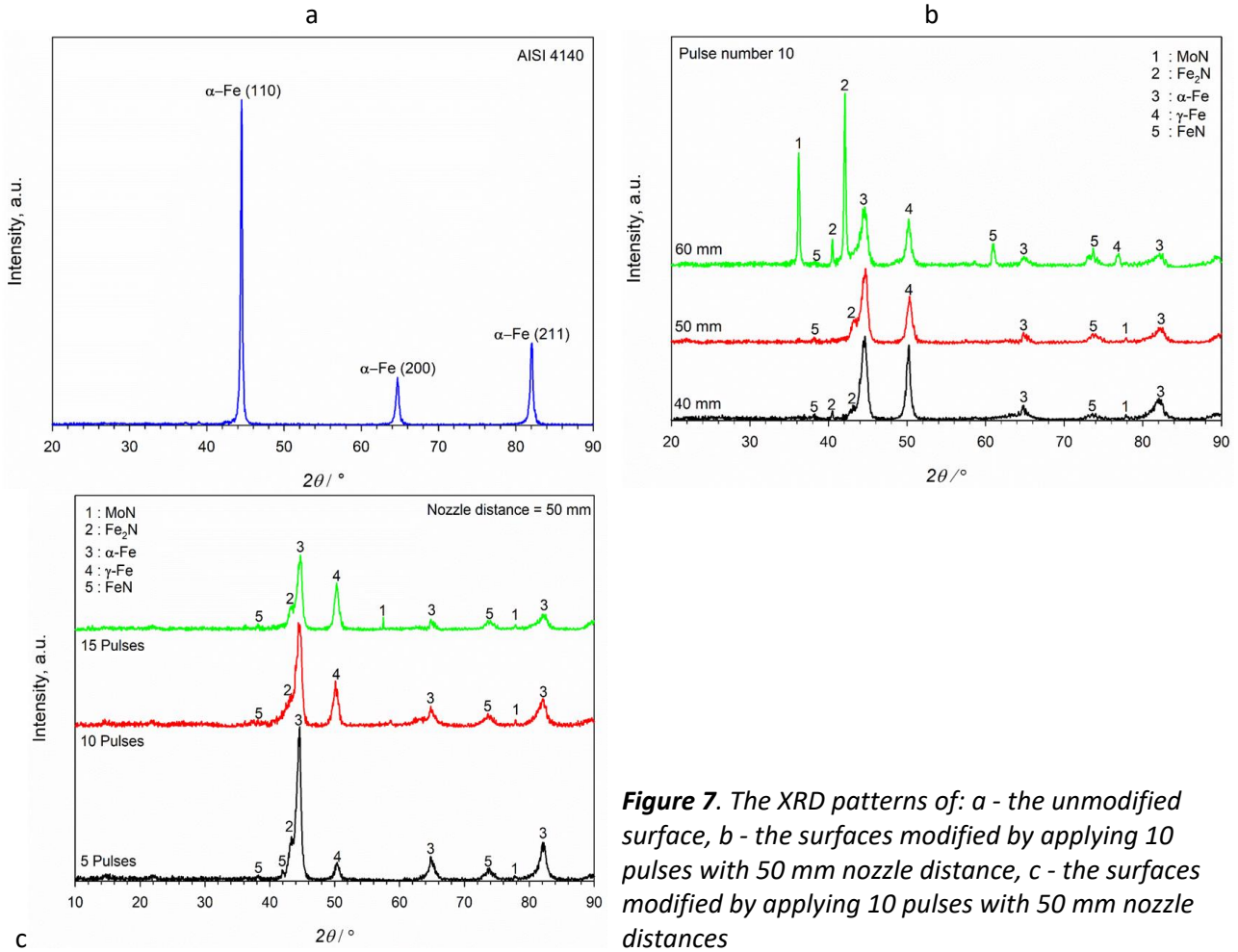

Figure 7*. The XRD patterns of: a - the unmodified surface, b - the surfaces modified by applying 10 pulses with 50 mm nozzle distance, c - the surfaces modified by applying 10 pulses with 50 mm nozzle distances*

As seen in Figure 7a, the unmodified sample consists of only the α-Fe phase having different planes. The XRD patterns of the surfaces modified by applying 5, 10, and 15 pulses with 50 mm nozzle distance given in Figure 7b show that pulse plasma treatment changes the diffraction patterns of the samples, and the new phases form. The modified surfaces contain the nitride precipitates such as Fe_2N, FeN,

and MoN, besides α-Fe and γ-Fe. It is seen that while the intensity of α-Fe phase decreases, the intensity of γ-Fe phase and new phases occurred, increase. It is known that molybdenum, one of the new phases formed in the surface structure, is entered into the surface from the consumable electrode material [19]. It is known that the growth of the molybdenum nitride phase and austenite in the analyzed layer results from a deeper penetration of molybdenum and nitrogen into the bulk material and the increased carbon concentration, respectively [16].

Similar results are also seen when nozzle distance increases (Figure 7c). However, while the intensity of α-Fe and γ-Fe phases decreases, the intensity of the nitride-based phases increases as the nozzle distance increases. The increase in the amount of nitride-based phases depending on the increase in nozzle distance, may be due to nozzle focusing or recrystallization problems that may occur at smaller distances [5]. At the same time, the diffraction peaks are seen to widen. The broadening of the diffraction peaks with increased nozzle distance is an indicator of crystalline imperfections like grain boundary increased by small grain size and microstrain [15,18].

Hardness of the samples

It was determined that while the hardness value of the unmodified sample is 200 Hv, the hardness values of the modified samples change between 530 and 1050 Hv depending on applied process parameters. The surface hardness enhancement is mainly due to the increase of the nano-size grains, new phases, and individual columnar structure, which has dense structure [16-18].

The first reason for the increase in hardness values of the samples is grain size reduction due to the increased cooling rate within the cycles of pulses [17,18]. There are other reasons that cause grain size reduction, except for the cooling rate. The pulse plasma causes an increase in the energy accumulation and promotes grain growth. The surface layer stores too much energy due to the increased pulses. The evaporation becomes so intense that the outermost layer removes. In this case, new grains would be nucleated and grow up. Simultaneously, the great thermal stress accumulated with the repeated irradiation of the surface would also be played a significant role in inducing grain refinement.

Guo *et al.* [20], who observed the formation of a modified layer, reported that rapid heating and solidification promoted heavy plastic deformation, which caused the formation of the dislocation cells by pulse plasma treatment. They stated that the formation of the nano-austenite structure might be attributed to the dissolution of the initial carbide particles and the subsequent stabilization of the γ-phase due to the increased carbon concentration. These effects are also among the factors that increase the hardness.

The hardness value variations of the modified surfaces by applying 5, 10, and 15 pulses with 50 mm nozzle distance were presented in Figure 8a. It is seen that the hardness values of the modified surfaces increased with increasing pulse numbers. Hao reported that the increase of the pulse number or the energy density absorbed by the surface leads to an increase in the microhardness values [5,7]. They stated that the number of pulses was increased during the crystallization of the surface layer, which was beneficial in increasing the nucleation rate and advanced non-spontaneous nucleation. The greater the pulse numbers, the finer the grains become [16], and the hardness increases.

The hardness value changes of the modified surfaces by applying 15 pulses with 40, 50, and 60 mm nozzle distances were presented in Figure 8b. It is seen that the hardness values of the modified surfaces increase as the nozzle distance increases. This result could be explained by partial annealing taking place at the structure because of heating of the surface by pulses ignited close to the surface.

Also, process parameters affect the microstructure, and some new phases and structural transformations occur in the modified surface. The amount of these strong new phases precipitated in the matrix phase and structural transformations lead to an increase in the hardness value of the modified samples.

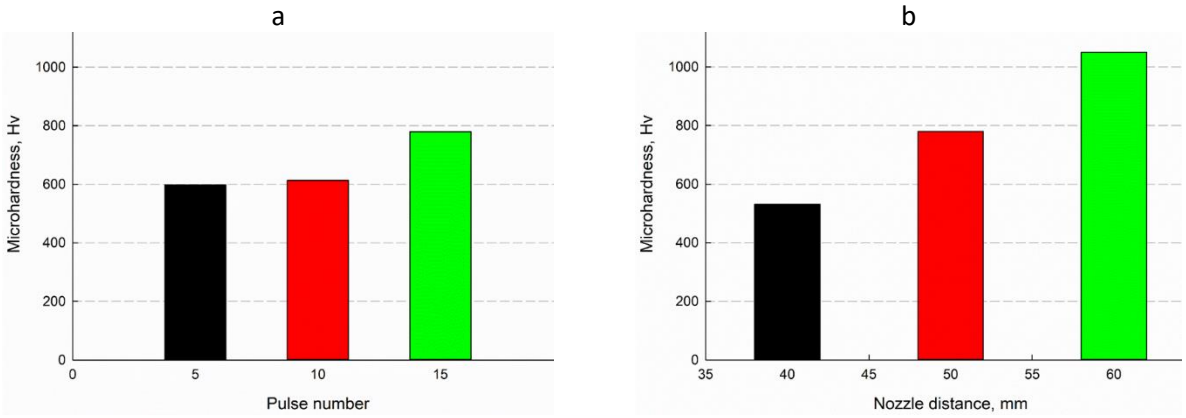

***Figure 8**. The hardness value variations of the modified surfaces as depending on a - pulse number, b - nozzle distance*

Corrosion behavior of the samples

The potentiodynamic polarization curves of the unmodified surface and the surfaces modified with different pulse numbers are given in Figure 9a. In scan range from -1 to +1 V, while passivation does not occur at the surfaces modified by applying 15 pulses with 40 mm nozzle distance and substrate, in the modification that is not very significant is seen passivation at the surfaces modified by applying 5 pulses. The occurred passivation is not stable. Figure 9b shows Tafel curves which contain cathodic and anodic polarization curves of the unmodified and the surfaces modified by applying 15 pulses with different nozzle distances. Although the scan range is extensive range from -1 to +1 V, no passivation at no samples is observed.

The corrosion current was found by the Tafel extrapolation method applied to Tafel region of anodic and cathodic polarization curves in the *E* versus log *I* plots. The found values were used to calculate the corrosion rate (Equation 1). The E_{corr}, I_{corr}, and R_{corr} values, which specify the samples' corrosion behavior, are listed in Table 3. As expected (Equation 1), the corrosion rate increases as the corrosion current increases. It is seen that the modified surfaces' corrosion rate is lower than AISI 4140 substrate, and a significant improvement in the corrosion resistance takes place. Pulse plasma parameters affect to corrosion behavior of the surfaces. The reason for the improvement in the corrosion resistance of the modified surfaces is microstructural changes, not passivation (Figure 9). The pulse plasma leads to homogenization of the surface layer melted and the formation of supersaturated solid solution, which enhances the corrosion resistance of the modified sample [15,18-21]. The modified surfaces contain the nitride precipitates such as Fe_2N, FeN, and MoN. As the pulse number increases, the amount of nitride-based phases formed increases. It is evident that these phases having homogeneous distribution will provide resistance to corrosion. As a matter of fact, as shown in Table 3 and Figure 10a, the corrosion current reduces with increasing pulse numbers, and the corrosion rate depending on the corrosion current, decreases. As seen in Figure 10b, the corrosion current and corrosion rate depending on the corrosion current, increase with increasing nozzle distance. We think that the reason for the corrosion rate that increases with the nozzle distance is the increase in the amount of nitride-based phases that will create a cathodic effect. While nitride-based phases provide resistance to corrosion up to a certain amount, they

accelerate corrosion above a certain amount. The reason for this is explained in the section on microstructural investigations of the corroded surfaces below [20,21].

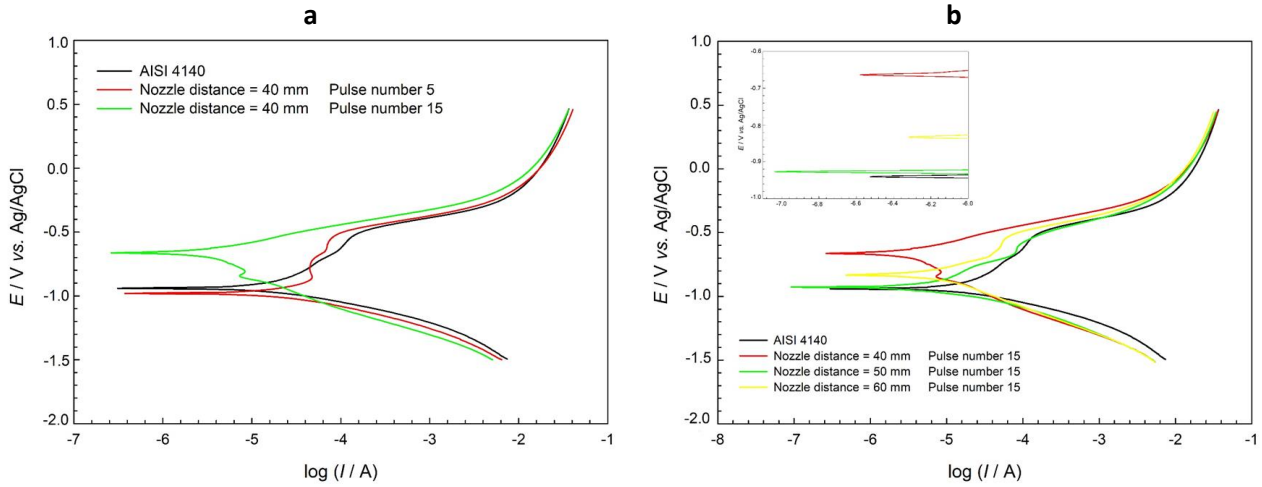

Figure 9. *The potentiodynamic polarization curves of a - the unmodified surface and the surfaces modified by different pulse numbers, b - the unmodified surface and the surfaces modified by different nozzle distances*

Table 3. *Potentiodynamic polarization test results of the corroded surfaces*

Nozzle distance, mm	Pulse number	E_{corr} / mV ± SD	I_{corr} / µA ± SD	R_{corr} / mm year^{-1} ± SD
40	5	-981±6	11.13±0.831	0.164±0.016
40	15	-661±4	3.116±0.664	0.046±0.015
50	15	-926±5	6.615±0.830	0.097±0.012
60	15	-831±8	9.696±1.031	0.143±0.015
AISI 4140	-	-940±5	20.57±0.220	0.303±0.003

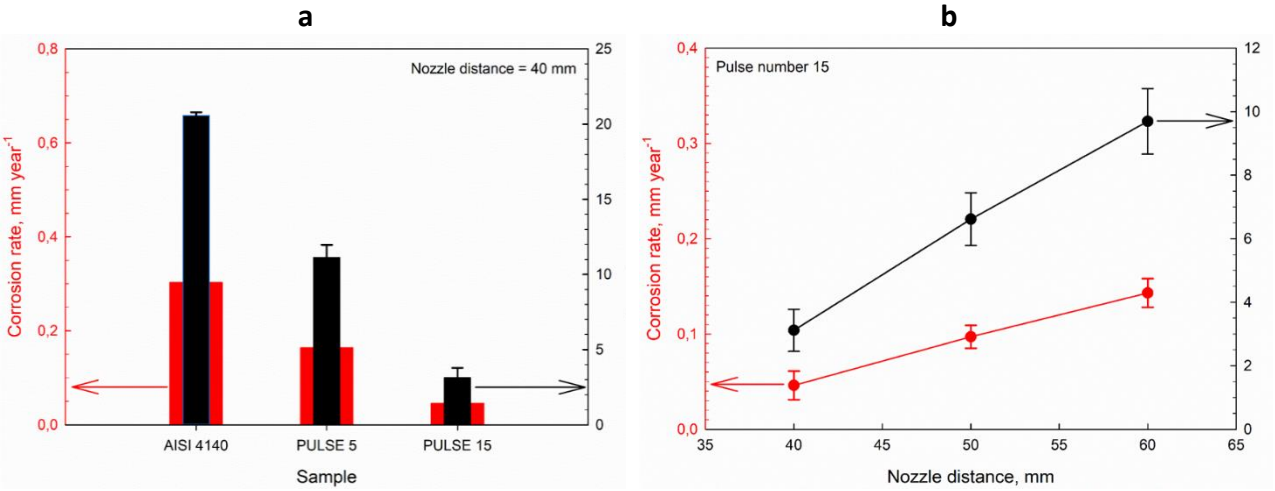

Figure 10*. Change in corrosion rate and corrosion current depending on a - pulse number, b - nozzle distance*

The SEM micrographs of some corroded surfaces are presented in Figure 11. Micro-cracks starting and extending along grain boundaries at the unmodified surface (Figure 11a) observed. Intergranular corrosion formed by the dissolution of grain boundaries has occurred on the unmodified surface. It is known that intergranular corrosion, also named intergranular attack, occurs when the grain boundaries of the material are more sensitive than inside of grain in a corrosive medium. The pittings formed on the modified surfaces draw attention in Figure 11b-c, and

it is seen that pitting corrosion has occurred. There are various causes of pitting corrosion formation. One of the formation causes of pitting corrosion is also that in multi-phase materials, some phases act as cathodes and some phases as anodes [17-21]. This situation creates a galvanic effect. When the cathode is large and the anode is small, the anode phase dissolves, occur cavities or holes. In the modified structure, nitride-based phases will act as the cathode, and Fe will serve as the anode. Large current density will occur on Fe, and Fe will corrode rapidly. In addition, cracks and rarely porous structures were also observed on the modified surfaces from place to place.

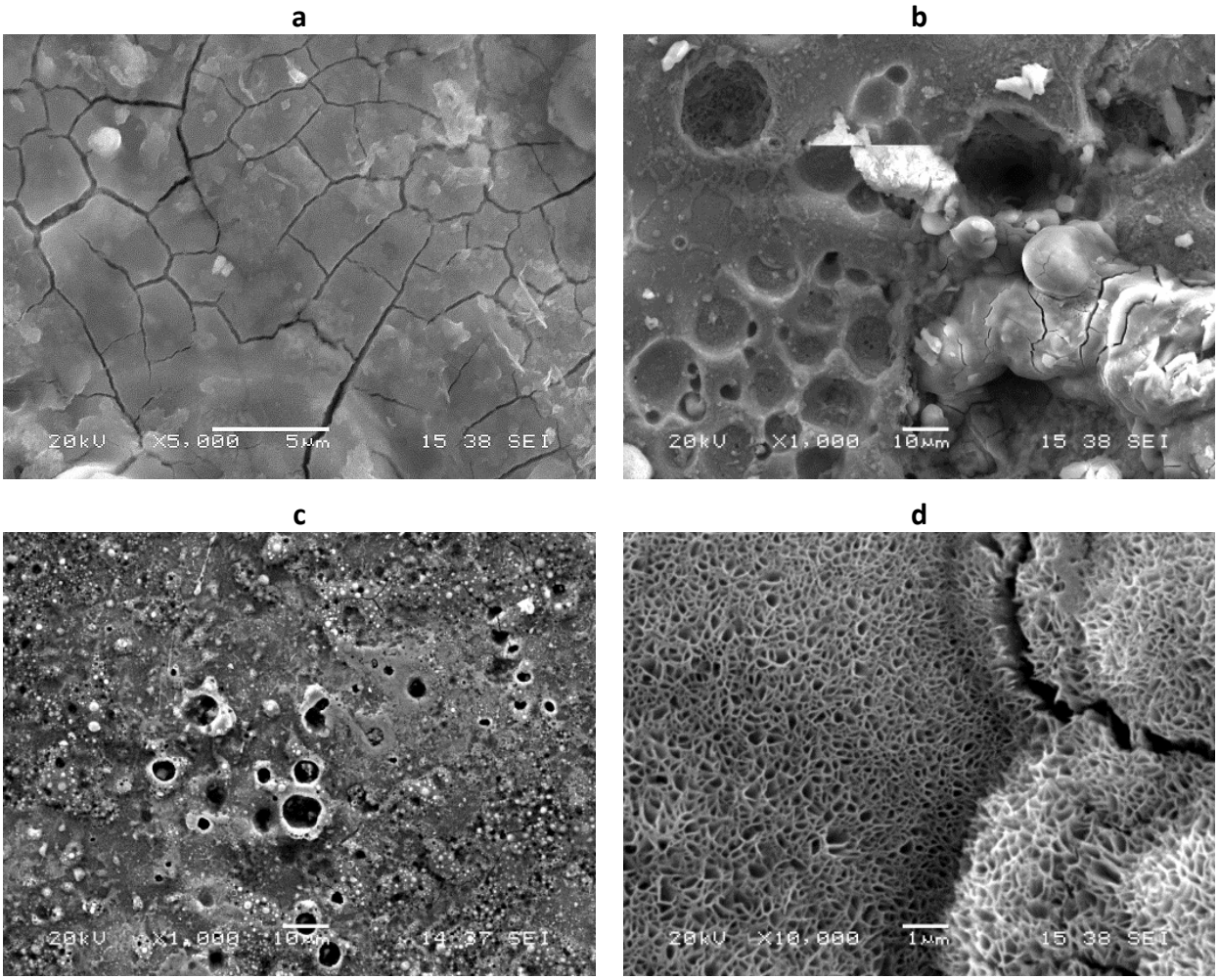

Figure 11. *SEM micrographs of the corroded surfaces: a - substrate, b - the surface modified by applying 15 pulses with 40 mm nozzle distance, c - the surface modified by applying 10 pulses with 60 mm nozzle distance, d- rarely porous structures observed from place to place on the modified surfaces*

Conclusions

In this study, the microstructure, hardness, and corrosion properties of AISI 4140 steel modified by pulse-plasma treatment performed by applying different parameters were investigated. The modification process was realized in short times with a relatively simple operation. Due to high power energy and thermal effects, morphological changes on the steel surface have occurred. A modified layer on the steel has been observed that consists of two layers, the compound layer and the diffusion layer. The structure and thickness of the modified layer affect by pulse number and nozzle distance. The fine grains, dendritic structures, and new phases such as Fe_2N, FeN, MoN, and γ-Fe in the modified layer occur. The amount of these new phases increases with the rising of pulse numbers and nozzle distance. In this same way, hardness values of treated samples also change by

pulse number and nozzle distance and increase with the rising of pulse numbers and nozzle distance. While the hardness value of the unmodified sample is 200 Hv, the hardness values of the modified samples change between 530 and 1050 Hv depending on applied process parameters. The hardness value of the treated sample has risen about 4-5 times that of the untreated. In general, the pulse plasma treatment has improved the corrosion resistance of treated samples. The reason for this improvement has been attributed to the formed new nitride-based phases. However, while nitride-based phases provide resistance to corrosion up to a certain amount, they accelerate corrosion above a certain amount. It is thought that in the modified structure, nitride-based phases act as the cathode, and Fe serves as the anode. A large amount of cathode produces a large current density on Fe, and Fe corrodes rapidly. It was observed that while intergranular corrosion has formed on the unmodified surface, pitting corrosion has appeared on the unmodified surfaces.

References

[1] M. W. Dewana, J. Lianga, M. A. Wahaba, A. M. Oke, *Materials and Design* **54** (2014) 6-13. https://doi.org/10.1115/IMECE2012-85889
[2] N. Y. Tyurin, O. V. Kolısnıchenko, N. G. Tsygankov, *The Paton Welding Journal* **1** (2001) 38-43. https://patonpublishinghouse.com/tpwj/pdf/2001/tpwj200101all.pdf
[3] B. Sartowska, J. Piekoszewski, L. Wali, M. Kopcewicz, Z. Werner, J. Stanislawski, J. Kalinowska, F. Prokert, *Vacuum* **70** (2003) 285-291. https://doi.org/10.1016/S0042-207X(02)00656-5
[4] B. Sartowska, J. Piekoszewski, L. Waliś, J. Senatorski, J. Stanisławski, R. Ratajczak, L. Nowicki, M. Kopcewicz, F. Prokert, M. Barlak, *Surface&Coatings Technology* **201** (2007) 8295-8298. https://doi.org/10.1016/j.surfcoat.2006.01.088
[5] S. Hao, B. Gao, A. Wu, J. Zou, Y. Qin, C. Dong, J. An, Q. Guan, *Nuclear Instruments and Methods in Physics Research B* **240** (2005) 646-652. https://doi.org/10.1016/j.nimb.2005.04.117
[6] V. M. Anishchika, V. V. Uglova, V. V. Astashynskia, V. M. Astashynski, S. I. Ananinb, E. A. Kostyukevich, A. M. Kuzmitski, N. T. Kvasovc, A. L. Danilyuk, I. N. Rumiancev, *Vacuum* **23** (2003) 269-274. https://doi.org/10.1016/S0042-207X(02)00654-1
[7] B. Podgornik, J. Vižintin, *Surface Engineering* **17** (2001) 300-304 https://doi.org/10.1179/026708401101517917
[8] Y. X Zhang, B. Bai, L.Chen, Z. Long, R. W. Li, *Optics and Laser Technology* **67** (2015) 57-64. https://doi.org/10.1016/j.optlastec.2014.09.012
[9] J. X Zou, K. M Zhang, S. Z Hao, C. Dong, T. Grosdidier, *Thin Solid Films* **519** (2021) 1404-1408. https://doi.org/10.1016/j.tsf.2010.09.022
[10] B. N. Mordyuk, Yu. V. Milman, M. O. Lefimov, G. I. Prokopenko, V. V. Silberschmidt, M. I. Danylenko, A. V. Kotko, *Surface &Coating Technology* **202** (2008) 4875-4883. https://doi.org/10.1016/j.surfcoat.2008.04.080
[11] Y. Y. Ozbek, *Journal of Materials Research and Technology* **9** (2020) 2176-2185. https://doi.org/10.1016/j.jmrt.2019.12.048
[12] E. Kocaman, B. Kılınç, M. Durmaz, Ş. Şen, U. Şen, *Engineering Science and Technology* **24** (2021) 533-542. https://doi.org/10.1016/j.jestch.2020.08.003
[13] A. Buranawong, N. Witit-Anun, S. Chaiyakun, A. Pokaipisit, P. Limsuwan, *Thin Solid Films* **519** (2011) 4963-496. https://doi.org/10.1016/j.tsf.2011.01.062n
[14] Y. Y Ozbek, C. Sarioglu, M. Durman, *Vacuum* **106** (2014) 11-15. https://doi.org/10.1016/j.vacuum.2014.03.001
[15] Y. Y Özbek., H. Akbulut, M. Durman, *Vacuum* **122** (2015) 90-94. https://doi.org/10.1016/j.vacuum.2015.08.017

[16] Y. Y. Özbek, M. Durman, H. Akbulut, *Tribology Transaction* **52** (2009) 213-222. https://doi.org/10.1080/10402000802369721
[17] C. S. Zhang, M. F. Yan, Z. Sun, Y. X. Wang, Y. You, B. Bai, L. Chen, Z. Long, R.W. Li, *Applied Surface Science* **315** (2014) 28-35. https://doi.org/10.1016/j.apsusc.2014.07.093
[18] X. Cheng, S. Hu, W. Song, X. Xiong, *Applied Surface Science* **286** (2013) 334-343. https://doi.org/10.1016/S0169-4332(01)00403-2
[19] H. Wang, Q. Yuan, L. Chai, K. Zhao, N. Guo, J. Xiao, X. Yin, B. Tang, Y. Li, S. Qiu, *Nuclear Engineering and Technolog* **54** (2022) 1972-1981. https://doi.org/10.1016/j.net.2021.12.030
[20] Z. Huang, Z. X. Guo, L. Liu, Y. Y. Guo, J. Chen, Z. Zhang, J. Li, Y. Li, Y. W. Zhou, Y. S. Liang, *Surface and Coatings Technolog*y **405** (2021) 126689. https://doi.org/10.1016/j.surfcoat.2020.126689
[21] D. Guo, P. Zhang, W. Song, B. Zhang, K. Peng, *Surfac and &Coatings Technology* **415** (2021) 127129. https://doi.org/10.1016/j.surfcoat.2021.127129